Bending Effects on Structural Dynamic Instabilities of Transonic Wings

N D Malmuth* and S R Chakravarthy*
Rockwell International Science Center, Thousand Oaks, California
J D Cole†
Rensselaer Polytechnic Institute, Troy, New York
and
T P Goebel*
Rockwell International North American Aircraft Operations, El Segundo, California

Nonclassical flutter has been observed during transonic conditions associated with flight and wind tunnel testing of various fighter and bomber aircraft As contrasted with classical flutter the underlying mechanism has been ascribed to a phase lag between lift variations and wing motions Based on the observations that the wing oscillations were restricted to bending mode shapes similar to the free fundamental, the phenomenon was idealized as the lift induced forced oscillation of a cantilever beam simulating the wing. Coupling with the aerodynamics occurs through the beam equation forcing term, representing the lift, and the tangency boundary condition for the unsteady transonic small disturbance equation for the latter Strip theory has been used with a suitably revised version of LTRAN2 to supply the aerodynamic input The resulting time integration algorithm provides a procedure to determine the destabilizing effects of sweepback Computations with the method closely predict flutter frequencies observed for the HiMAT canard during wind tunnel testing, as well as for the B-1 wing in flight tests in two out of three cases Qualitative behavior of the oscillation agrees for these conditions For the third case, damped oscillations are predicted rather than the amplified ones observed Reasons for the discrepancy are provided, involving the second bending mode of these oscillations in contrast to the fun damental assumed by the current approach Specific recommendations for refinements of the procedure in volving inclusion of modal coupling analysis of limit cycle aspects and three dimensional phenomena are given

Nomenclature

A = angle-of attack similarity parameter
A_l = temporal modulation of spatial mode
b = span
B = reduced span
$\mathfrak{B}$ = body shape
c = local chord
c_R = root chord
$\bar{E}$ = dimensional modulus of elasticity
E_R = modulus of elasticity at wing root
EI = dimensionless spanwise stiffness distribution $= \bar{E}\bar{I}/E_R I_R$
F_{ul} = wing shape function
h = normalized wing deflection
$\bar{I}$ = dimensional moment of inertia
I_R = moment of inertia at wing root
k = reduced frequency $= \omega U/c_R$
K = transonic similarity parameter
$\bar{l}$ = modal projection of spanwise load
$\bar{L}$ = dimensional spanwise lift distribution
$\tilde{L}$ = normalized spanwise load [in planes parallel to the freestream if $\psi = 0(\delta^{1/3}) << 1$] $= \bar{L}/\rho U^2 \delta^{2/3} c_R$
$\bar{m}$ = dimensional mass per unit length
$\tilde{m}$ = dimensionless spanwise distribution of wing mass per unit length $= \bar{m}/m_R$
M_∞ = freestream Mach number
q = dynamic pressure
$\tilde{t}$ = $(c_R/U)t$
t = normalized time
$\bar{t}$ = scaled time $= \delta^{2/3} t$
$\bar{x}\ \bar{y}, \bar{z}$ = dimensional Cartesian coordinates
$x\ y\ z$ = normalized Cartesian coordinates in units of c_R
$\tilde{x}\ \tilde{y}\ \tilde{z}$ = scaled Cartesian coordinates
U = freestream velocity
$\tilde{W}(\tilde{z}\ \ \tilde{t})$ = normalized wing deflection $= h\delta^{2/3} = \bar{y}/c_R \delta^{1/3}$
$\alpha\ \alpha_0$ = angle of attack
δ = thickness ratio at root
δ_{ij} = Kronecker delta
$= 1,\ i = j$
$= 0\ \ i \neq j$
ϵ = initial velocity $= \dot{A}_l(0)$
λ = stiffness/aerodynamic force ratio
Π_1 = $E_R I_R \delta^{2/3} \cos^5\psi/\rho U^2 c_R^4$
Π_2 = $m_R \delta^{2/3} \cos\psi/\rho c_R^2$
ρ = freestream density
ϕ = perturbation potential
Φ = velocity potential
χ = $\sin\psi/\delta^{1/3}$
ψ = sweepback angle of elastic axis
ω = normalized frequency

Subscripts

l = lower surface
LE = leading edge
R = root
TE = trailing edge
u = upper surface

Presented as Paper 83 0920 at the AIAA/ASME/ASCE/AHS 24th Structures Structural Dynamics and Materials Conference, Lake Tahoe, Nev May 2 4 1983; received Sept 27 1983; revision received June 7 1984

*Member of Technical Staff.
†Professor

Superscripts

n = time level

Special Symbols

[ ] = jump

$(\bar{\ })$ = dimensional quantity

Introduction

STRUCTURAL instabilities such as flutter and aileron buzz represent some of the most persistent and difficult problems associated with transonic flight As in the linear case such self excited oscillations are brought about by circumstances in which aerodynamic forces associated with the motion of the surface can do positive work on it during a vibratory cycle However, the origin of the phenomenon which we term hereinafter "nonclassical flutter, ' in the transonic regime can arise because of a phase lag between the displacement of the system and the forces and moments due to shock wave motions or other nonlinear phenomena The extent to which viscous flow features come into play depends on the Reynolds number separation producing adverse pressure gradients, and surface roughness Only a single degree of freedom of the structure may be prominently in volved in this motion In the linear regime the classical flutter phenomenon by contrast, generally involves coupling be tween several degrees of freedom of the structure and can occur in a clean potential flow

Nonclassical transonic flutter has been experienced during Rockwell's flight and wind tunnel tests of bomber and fighter aircraft As detailed in Refs 1 4 the first documented oc currence of the phenomenon was in September 1977 on the HiMAT 0 22 scale aeroelastic model in Rockwell's Trisonic Wind Tunnel at negative angles of attack below -3 8 deg at a test Mach number of 0 95 (Fig 1a) A trace associated with a similar instability occurred during flight test and wind tunnel tests on the B 1 (Fig 1b) Although both of those instances resulted in angle of attack limits on the aircraft during transonic fight, the limitations have not impacted the B 1 or HiMAT mission requirement For the HiMAT movies taken vividly illustrate the nature of the nonclassical flutter described previously These records graphically demonstrate the hysteretic divergent bending oscillations asociated with the trace of Fig 1a.

Despite the fact that the B 1 and HiMAT mission per formance has not been affected by this phenomenon it may be of significant concern for future vehicles

Because of the potential associated danger, it is crucial that methods be developed to identify the factors contributing to such instabilities Once these are isolated it is necessary to discover corrective procedures that can eliminate them

Probably the earliest structurally coupled nonlinear model that properly simulated the effect of phase lags on transonic flutter by modern computational methods was the work of Ballhaus and Goorjian in Ref 5 Therein a simple linear oscillator simulating pitch oscillations of a transonic airfoil was coupled to aerodynamic forcing moments generated by a time integration procedure (LTRAN2) Positive damping was allowed in the linear oscillator and was selectively changed to achieve damped, neutral and divergent pitching oscillations about a steady state airfoil angle of attack For a suitable orientation of the phase lag between the lift and the airfoil pitching response, it was possible to determine damping for neutral stability by a linearization assuming that the oscillations represented small harmonic perturbations about a steady state mean deflection However this assumption may be invalid in practically interesting transonic cases and could preclude important relevant physics such as limit cycle phenomena and relaxation oscillations

Generalization of the pure pitching model to include plunge replicating two degree of freedom torsion bending of a two dimensional idealization of a wing was given by Yang et al in Ref 6 A qualitative treatment of sweepback within a similar two degree of freedom framework was given by Isogai [7] In that model inertias and other parameters for the two-degree of freedom idealization were apparently selected on a qualitative basis to achieve some simulation of the characteristics of a swept wing Beyond this the mode of choice of these quantities did not appear to depend on any precise quantitative set of guidelines

Borland and Rizzetta[8] combined a three dimensional generalization of LTRAN2 with a dynamic model to study transonic flutter phenomena of wings The computations employed appeared to be extensive Within this framework effort is underway to provide more efficient and accurate algorithms to achieve high quality answers more quickly by using improvements in the numerical methods and for mulation Work is also being performed to treat the three dimensional case using a full potential model

Phase lag phenomena leading to flutter and implicitly incorporated in the previous numerical models have been discussed by Ashley in Ref 9 in connection with the role of the shock motions Other interesting unsteady shock effects haye been described by Tijdeman[10] in connection with oscillating flaps

Although these investigations, with the exception of Ref 8 provide valuable insight into the role of nonlinear aerodynamics in transonic flutter of airfoils predominantly, a need exists for a means of modeling swept wings that could explain the particular type of divergent oscillations observed on the HiMAT and B 1 An approximate procedure is desired that sidesteps the lengthy computations associated with the full three dimensional module used in Ref 8 but gives insight into the important instability mechanisms that can arise

Such an approach termed hereinafter the nonlinear coupled model (NCM), will be described in this paper Using aerodynamic strip theory based on a generalization of LTRAN2 and an idealization of the wing as a cantilever beam, a coupled simulation has been developed This model provides insight into the physical mechanisms controlling the instability Further, calculations reproduce qualitative features of the observed wing displacement histories for two cases

This paper will provide a description of the coupling procedure and relevant formulation Also presented are applications of the method to HiMAT and B 1 cases in which the nonclassical flutter phenomenon was observed as well as a description of the related aerodynamic environment Comparisons are given with wind tunnel and flight test results for these cases A simplified procedure to obtain a linear stability boundary exploiting the approximation of similar sections along the span is discussed in Ref 3 Also discussed therein is the destabilizing and stabilizing effect of sweepback and sweepforward, respectively

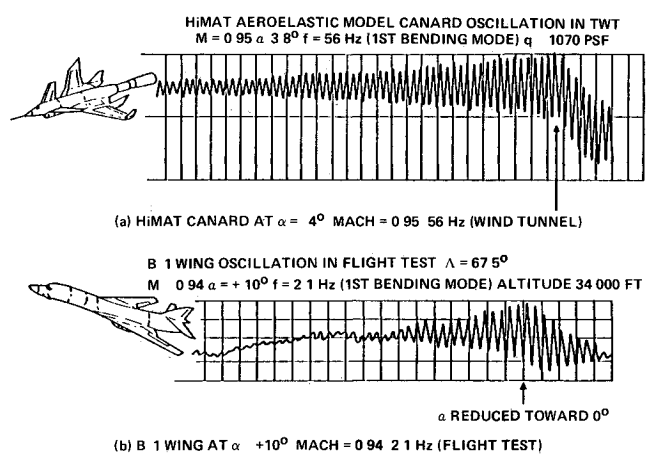

Fig 1 Shock induced airfoil oscillations on HiMAT and B 1

From the model, it will be evident that parameters such as Mach number angle of incidence shock location phase lag and strength, reduced frequency of oscillation dynamic pressure, and airfoil characteristics enter through basic lumped groupings appearing in the dimensionless formulation employed Results for B-1 and HiMAT wings are provided that give some indication of the effect of these parameters

Associated with these parametric studies is the discussion of the efficacy of elementary fixes such as tip masses and modifications of stiffness and inertial characteristics

To provide insight into the role of viscous effects, a rough simulation based on local flat plate similarity has been introduced into the aerodynamic module in Refs 3 and 4 The associated modifications of the divergent oscillations utilizing the coupled model are indicated therein

Formulation

Referring to Fig 2, bending oscillations of the wing shown are considered. Consistent with the discussion, we idealize the wing structure as a cantilever beam along the wing's elastic axis, with its mass distribution identical to that of the wing in planes parallel to the plane of symmetry of the latter, which is aligned with the freestream velocity vector The well known beam equation of motion (neglecting rotary inertias and structural damping) in nondimensional form, using transonically scaled independent variables appropriate to coupling with unsteady small disturbance theory is

$$\Pi_1 \frac{\partial^2}{\partial \tilde{z}^2}\left(EI\frac{\partial^2 \tilde{W}}{\partial \tilde{z}^2}\right)+\Pi_2 \tilde{m}\frac{\partial^2 \tilde{W}}{\partial \tilde{t}^2}=\tilde{L} \tag{1a}$$

The appropriate cantilever boundary conditions for Eq (5a) are

$$\tilde{W}_{\tilde{z}}(0\ \tilde{t})=\tilde{W}(0\ \tilde{t})=\tilde{W}_{\tilde{z}}(B\ \tilde{t})=\tilde{W}_{\tilde{z}\tilde{z}\tilde{z}}(B\ \tilde{t})=0 \tag{1b}$$

where $B=b\delta^{1/3}/c_R$

The quantity $\tilde{L}$ is evaluated from the solution of the unsteady small disturbance problem which is described next

Unsteady Small Disturbance Model

Denoting Φ as the velocity potential, we consider its asymptotic expansion in an unsteady small disturbance limit defined as

$$K=\frac{1-M_\infty^2}{\delta^{2/3}} \qquad A=\frac{\alpha}{\delta} \qquad \bar{y}=\delta^{1/3}y \qquad \tilde{z}\ x \text{ fixed as } \delta\to 0 \tag{2}$$

where M_∞ is the freestream Mach number; α is the angle of attack; and $x=\bar{x}/c_R \quad y=\bar{y}/c_R$, and $\bar{x}\ \bar{y}$ are the dimensional Cartesian coordinates shown in Fig 2

The asymptotic expansion for Φ is

$$\Phi/(Uc_R)=x+\delta^{2/3}\phi(x\ \bar{y}\ \tilde{z}\ \tilde{t}\cdot K\ A)+ \tag{3}$$

Substitution of Eq (3) into the exact equations gives to the dominant order the following unsteady small disturbance equation:

$$[K-(\gamma+1)\phi_x]\phi_{xx}+\phi_{\bar{y}\bar{y}}-2\phi_{x\tilde{t}}=0 \tag{4}$$

The appropriate flow tangency boundary conditions for Eq (4) are obtained from the following representation of the pure bending beam as a surface:

$$\mathfrak{B}(\bar{x}\ \bar{y}\ \tilde{z}\ \tilde{t})=0$$

where $\mathfrak{B}$ is given by

$$\mathfrak{B}=\bar{y}-\delta c_R[F_{u,l}(x\ z)-Ax+h(z\ \ t)]=0 \tag{5a}$$

with u and l signifying the upper and lower wing surfaces respectively and

$$z=x\sin\psi+z\cos\psi \tag{5b}$$

Equations (5) contain the crucial information regarding the role of sweepback in producing nearly pure pitch for large ψ and nearly pure plunge for small values of this parameter The phase lag aspects of this observation will become apparent subsequently Substituting Eqs (3) and (4) into the tangency boundary condition

$$\frac{\partial \mathfrak{B}}{\partial t}+\nabla\Phi\ \ \nabla\mathfrak{B}=0$$

leads to the following approximate condition

$$\phi_{\bar{y}}(x\ 0\ \tilde{z}\ \tilde{t})=\frac{\partial F_{u,l}}{\partial x}-A+\tilde{W}_{\tilde{t}}(\tilde{z}\ \tilde{t})+\chi\tilde{W}_{\tilde{z}}$$

$$0\le\tilde{z}\le B \qquad x_{LE}\le x\le x_{TE} \tag{6a}$$

In addition to Eq. (6a) the approximate condition expressing continuity of pressure across the wake is specified as

$$[\phi_x]\equiv\phi_x(x\ 0+\ \tilde{z}\ \tilde{t})-\phi_x(x\ 0-,\tilde{z}\ \tilde{t})=0 \qquad x>x_{TE} \tag{6b}$$

In addition to Eqs (6), a suitable far field for ϕ is utilized To achieve further simplification, the modal approximation

$$\tilde{W}(\tilde{z}'\ t)\approx\hat{W}_1(\tilde{z}\ )A_1(\tilde{t})=\tilde{W}_1(\tilde{z})A_1(\tilde{t}) \tag{7}$$

is employed in which $\hat{W}_1$ is the free fundamental mode As has been already noted for the small disturbance theory considered, we have implicitly assumed that $\psi=0(\delta^{1/3})$ so that $d/dz\approx d/d\tilde{z}$ Thus, the Sturm Liouville problem for $\tilde{W}_1$ is

$$(EI\tilde{W}_1'')''=\tilde{m}\omega_1^2\tilde{W}_1(\tilde{z}) \equiv\frac{d}{d\tilde{z}} \tag{8a}$$

$$\tilde{W}_1(0)=\tilde{W}_1\ \ (0)=\tilde{W}_1''(B)=\tilde{W}_1'''(B)=0 \tag{8b}$$

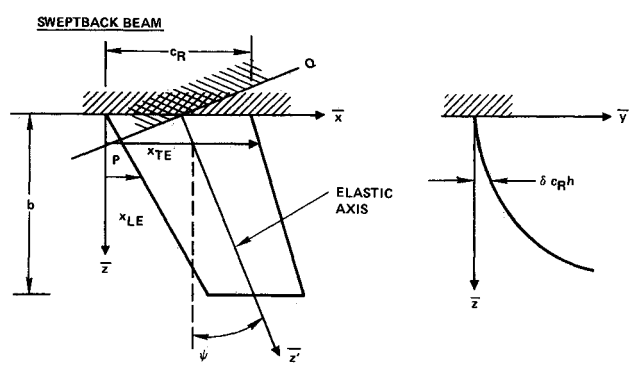

Fig 2 Beam idealization of sweptback wing

where the orthonormality relation for the eigenfunctions $\tilde{W}_k$ is

$$\int_0^B \tilde{m}\tilde{W}_l\tilde{W}_k \mathrm{d}\tilde{z} = \delta_{lk} \tag{9}$$

If, correspondingly we assume that the aerodynamic load $\tilde{L}$ has the composition

$$\tilde{L}(\tilde{z}\ \tilde{t}) = \Sigma\tilde{W}_k(\tilde{z})\tilde{l}_k(A_1\ A_2 \qquad \tilde{t}) \tag{10}$$

then taking the projection of Eq (1a) on the fundamental basis [i e , multiplying through by $\tilde{W}_l$ and integrating from 0 to B with respect to $\tilde{z}$, using Eq (9)] the following equation for A_l in Eq (7) is obtained:

$$\Pi_l\omega_l^2 A_l + \Pi_2\dot{A}_l = \int_0^B \tilde{L}(\tilde{z}\ \tilde{t})\, W_l(\tilde{z})\, c\,\mathrm{d}\tilde{z} \equiv \tilde{l}(\tilde{t}) \tag{11}$$

where c is the local chord at the $\tilde{z}$ span station in units of c_R; the dot signifies ordinary differentiation with respect to $\tilde{t}$; and ω_l^2 is the fundamental eigenfrequency of Eqs (8) From the formulation (4 6), L in Eq (11) is given by

$$\tilde{L} = \sec\psi \int_{x_{LE}}^{x_{TE}} [\phi_x]\,\mathrm{d}x \approx \int_{x_{LE}}^{x_{TE}} [\phi_x]\,\mathrm{d}x = [\phi]_{TE} \tag{12}$$

The appropriate specialization of Eq (6) resulting from the modal approximation (7) is

$$\phi_{\bar{y}}(x\ 0\ \tilde{z}\ \tilde{t}) = \frac{\partial F_{u,l}}{\partial x} - A + \chi W_l\ (\tilde{z})A_l + \dot{A}_l\tilde{W}_l \tag{6a}$$

Equation (6a) clearly shows the role of the sweep parameter χ in relating the plunge induced out of phase component $\sim\dot{A}_l$ to the in phase component term $\sim A_l$ arising in pitch *From this feature a mechanism can be clearly seen to modify the phase lag relationship between the lift and motion as a function of sweepback and thickness ratio This is particularly potent on a variable sweep airplane such as the B 1*

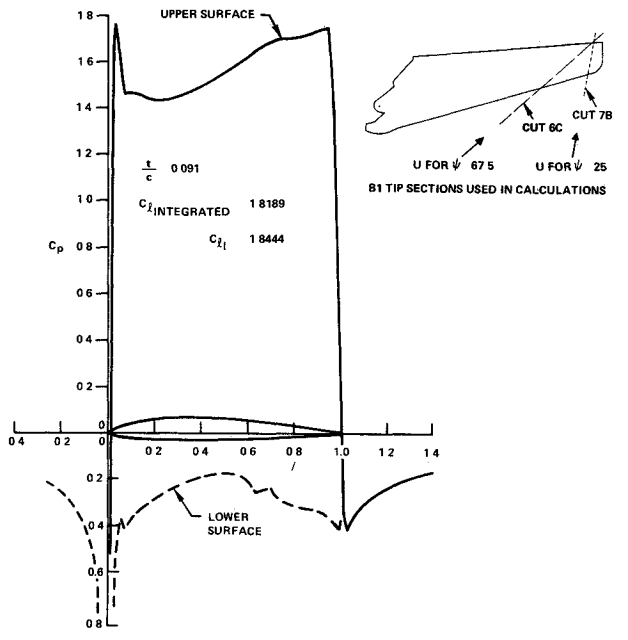

Fig 3 Pressure distribution B 1 tip airfoil chordplane: ψ = sweep back angle = 25 deg; cut 7B; $M_\infty = 0\ 73$; $\alpha = 2\ 5$ deg; $t/c = 0\ 091$; $C_{l\ \text{integrated}} = 1\ 8189$; $C_{l_T} = 1\ 8444$

From the foregoing formulation the coupling between the aerodynamics and dynamics is clearly evident Equation (11) can be regarded as an integrodifferential equation for A_l through the solution of Eq (4) subject to Eq (6a) among the other boundary conditions However Eq (6a′) itself involves A_l and $\dot{A}_l$

To complete the formulation we require initial conditions Appropriate ones are

$$A_l(0) = 0 \tag{13b}$$

$$\dot{A}_l(0) = \epsilon \tag{13c}$$

where ϵ is to be selected to be sufficiently small to be consistent with the small disturbance approximations already employed

Description of Numerical Procedure and LTRAN2 Modification

Synopsis of Implementation

LTRAN2 solves problems for Eq (4), in which the sum of the last two terms in Eq (6a) is a prescribed function of $\tilde{t}$ only This gives the ϕ field corresponding to a forced oscillation of an airfoil To treat the new coupled problem described in the previous section suitable modifications of LTRAN2 were made To achieve this Eq (11) is written as a system and discretized as follows:

$$\Pi_l\omega_l^2 A_l^\eta + \frac{\Pi_2}{\Delta\tilde{t}}(V_l^{\eta+1} - V_l^\eta) = \tilde{l}_l^\eta \tag{14a}$$

$$\frac{A_l^{\eta+1} - A_l^\eta}{\Delta\tilde{t}} = \frac{V_l^\eta + V_l^{\eta+1}}{2} \tag{14b}$$

In Eq (14) the superscript n signifies the old time level and $n+1$ the current one The numerical procedure is as follows:

1) The spatial mode shape function $\tilde{W}_l$ is determined from the solution of Eq (8) This eigenvalue problem was solved using fourth order Runge Kutta shooting

2) With the mode shape known, the quantity $\tilde{l}$ is computed (with the static part of it subtracted out and the assumption that the static rigid equilibrium position is an adequate approximation of its flexible value) For this purpose an initialization from a steady state case was employed To obtain $\tilde{l}$ five disk files are set up for each of five spanwise stations to be considered More spanwise stations could have been used for greater accuracy but to reduce computer costs this number was selected The store and restart options in LTRAN2 are exploited to compute each span station (one at a time for every time step) before structural coupling is carried out Subroutine MAIN of LTRAN2 has been modified to incorporate Eq (14) into the solution procedure Subroutine ALFATL has also been changed to employ Eq (6a) as the boundary condition

3) After every cycle of updating the aerodynamic solution at each of the span stations the value of $\tilde{l}_l^n$ was computed from

$$\tilde{l}_l^\eta = \int_0^B [\phi^n]_{TE}\tilde{W}_l(\tilde{t})\,\mathrm{d}\tilde{z} \tag{15}$$

4) This value was based in the next cycle of aerodynamic solutions using the modified LTRAN2 with Eqs (6a) and (14) built in

5) The procedure is continued until the solution has been generated at a sufficient number of time steps to obtain a satisfactory history of the motion

In the version of LTRAN2 utilized, a monotone switch procedure described in Refs 11 and 12 was implemented

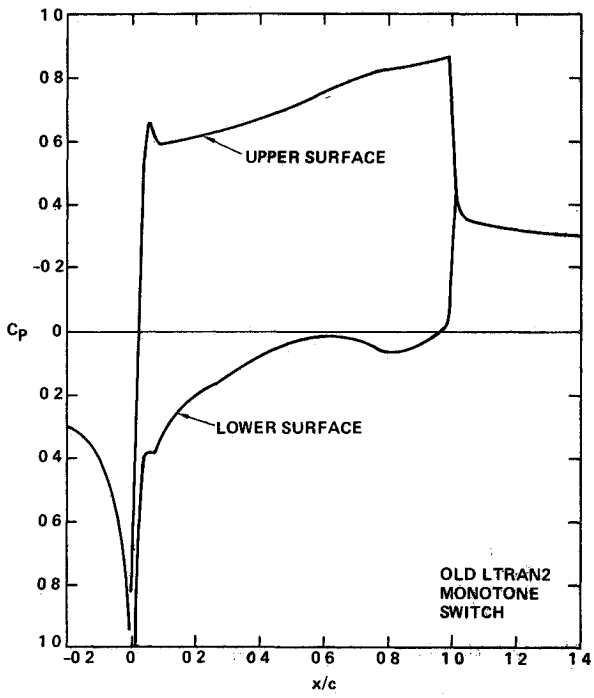

Fig 4 Pressure distribution B 1 tip airfoil chordplane: $\psi = 65$ deg; cut 6C; $M_\infty = 0.95$; $\alpha_o = 5\ 0$ deg; $t/c = 0\ 052$; $C_{l\ \text{integrated}} = 0\ 8113$; $C_{l_\Gamma} = 1.8245$.

Results and Discussion

Steady State Aerodynamic Environment

Prior to applying the NCM to the B 1 and HiMAT, the nature of the steady-state aerodynamic environment experienced by the B 1 airfoil will be indicated For these cases, the monotone switch of Refs 11 and 12 was utilized in the type sensitive differencing Steady B 1 chordwise pressures are shown in Figs 3 and 4 Corresponding HiMAT results are given in Refs 3 and 4 Figure 4 is associated with an oblique trailing shock on the upper surface, as contrasted to a strong normal shock occurring in the lower Mach number incident case of Fig 3 The two tip airfoils used for the B 1 cases of Figs 3 and 4 are shown in the inset of Fig 3 For unsteady calculations associated with Fig 3, no appreciable shock motion away from the trailing edge was observed ‡ This is significant with respect to correlations of phase lag of lift force and shock motion with respect to the airfoil motion, and the assertion that a divergence producing phase lag of the shock motion is necessary for an unstable phase lag for the lift This suggests the possibility of the instability phenomenon occurring without shock motion, since temporal variations of its strength or other nonlinear effects may be enough to create unstable lift phase lags

Results from Full Nonlinear Coupled Model

Correlation of Phase Lags

Before discussing computations with the nonlinear coupled model (NCM) formulated previously, results are given to illustrate the relationship of the phase lags between displacements and the lift, shock strength, and shock position for a harmonically pitching B 1 airfoil section Figure 5 illustrates this relationship for a relatively high frequency case in which the reduced frequency $k = 1$ Shown in the figure is

‡This contrasts with B 1 flight test observations where a localized region of 'unsteady pressures has been identified over the wing Therein pressure oscillations are believed to be associated with some shock movement away from the trailing edge inboard of the tip by J Stevenson S Dobbs and G Miller Three dimensional effects ignored by the strip theory employed herein are probably responsible for this difference

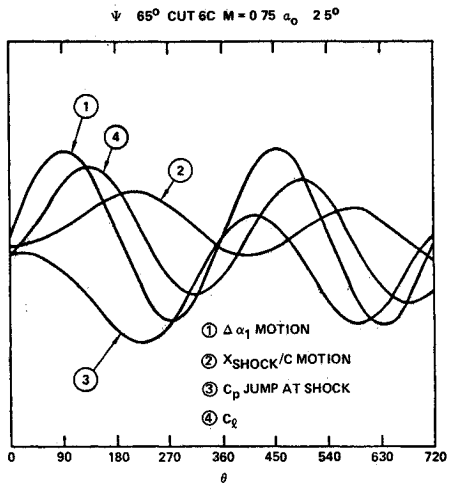

Fig 5 B 1 forced plunge sine wave oscillations: $\psi = 65$ deg; cut 6C; $M_\infty = 0.75$; $\alpha_0 = 2\ 5$ deg; $k = 1\ 0$

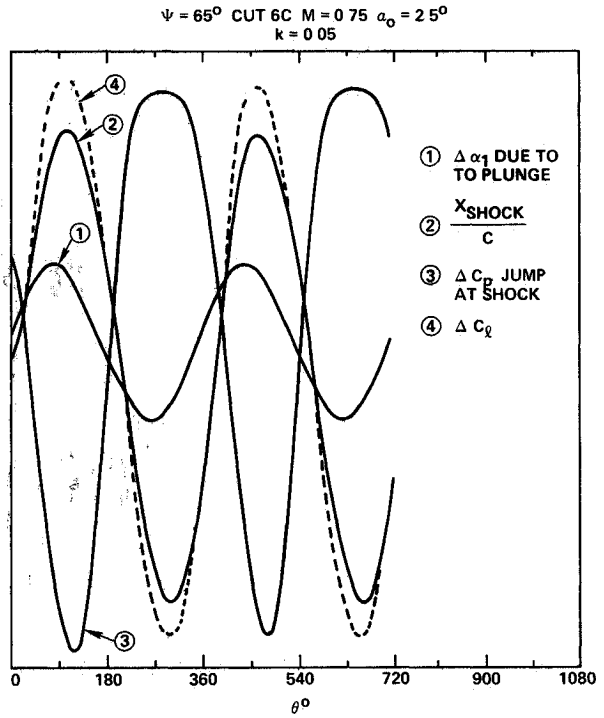

Fig 6 B 1 forced plunge sine wave oscillations: $\psi = 65$ deg; cut 6C; $M_\infty = 0.75$; $\alpha_0 = 2.5$ deg; $k = 0\ 05$.

the angle of-attack perturbation motion ($\Delta\alpha_I$), as well as histories of the shock position x_{shock}, shock strength (ΔC_p jump at the shock), and the sectional lift coefficient C_l Conditions indicated on the figure were evaluated for a sweepback angle $\psi = 65$ deg, angle of attack $\alpha_0 = 2\ 5$ deg, and Mach number $M_\infty = 0\ 75$ on a section corresponding to a normal cut to the elastic axis about two thirds semispan. Lack of correlation is evident among all four quantities for this case By contrast, a strong correspondence occurs at low frequencies, as exemplified in Fig 6 for $k = 0\ 05$. In Fig 7, the results for these extreme values of k are summarized on a plot of phase lag τ vs k Information is also provided for intermediate k values, as well as results using a generalization of the Duhamel method employed in Ref. 5 and implemented in this study The Duhamel method agrees well with the forced method Figure 7 corroborates the close correlation of the lift and shock phase lags at low k and the lack of correlation at large k at the indicated Mach number

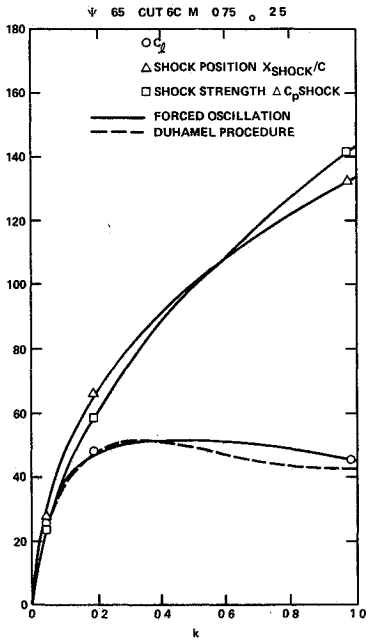

Fig 7 B 1 phase lags during plunge forced sine wave oscillations: $\psi = 65$ deg; $M_\infty = 0\ 75$; $\alpha_0 = 2\ 5$ deg

The significance of this observation is that it tends to support the part of the explanation for structural instabilities on the HiMAT and B 1, given in Refs 1 2 and 9 associated with identifying shock phase lags with lift phase lags However at $M_\infty = 0\ 95$, lift phase lags occurred with the shock nearly frozen at the trailing edge indicating that the hypothesis using the phase lag derived from the shock motion solely as the driver of the nonclassical flutter is questionable In fact the authors believe that the lift phase lags can be influenced by nonlinear effects other than the shock motion.

Application of NCM to B 1 and HiMAT Cases: Investigation of Potential Fixes and Parametric Studies

Using the NCM of the formulation section, structurally coupled calculations have been performed on the B-1 airplane wing with 25 and 67 5 degrees of leading edge sweep Two dimensional aerodynamic solutions obtained on tip airfoils cut in the freestream direction were assumed to be representative of the entire wings The orientation of these cuts is given in Fig 3 Actual wing structural stiffness and mass characteristics were used in calculation of wing first mode bending shapes Sectional wing aerodynamic loadings were adjusted for local chord variations The Π_1 and Π_2 parameters were calculated at the flutter points for the B-1 airplane wing and HiMAT wind tunnel canard When the Mach number was reduced for the B 1, Π_1 was held constant; this is equivalent to keeping the same structure and flying at a lower altitude to maintain the same dynamic pressure Π_2 was then adjusted to reflect the lower altitude When this Mach number reduction procedure gave an altitude below 10 000 ft the altitude was held at 10,000 ft and Π_1 and Π_2 were adjusted accordingly

In all of the structurally coupled calculations to be discussed here, $\epsilon = 0\ 05$ in Eq (13b). In addition, the static flexible lift is assumed to be approximated on the flutter speed boundary by the static rigid value Yates[13] and Edwards[14] have indicated important effects related to relaxing this assumption These should be studied in refinements of this analysis

Cases in which the aerodynamic damping is sufficient to give damped structurally coupled oscillations are shown in Figs 8 10 Figures 8 and 9 are two B 1 subcritical conditions

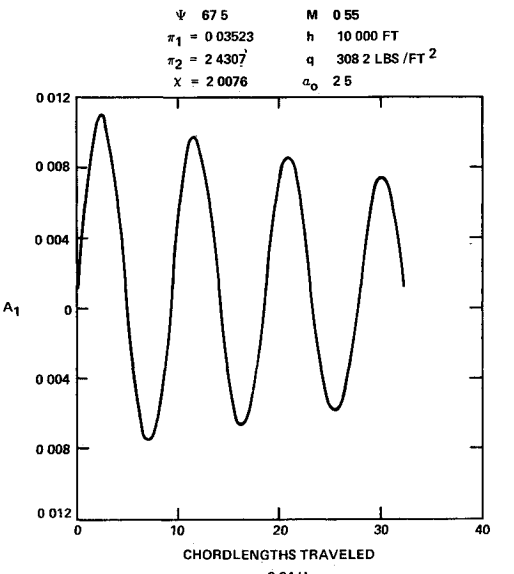

Fig 8 B 1 structurally coupled calculation: $\psi = 25$ deg; $M_\infty = 0\ 55$; $\alpha_0 = 2\ 5$ deg.

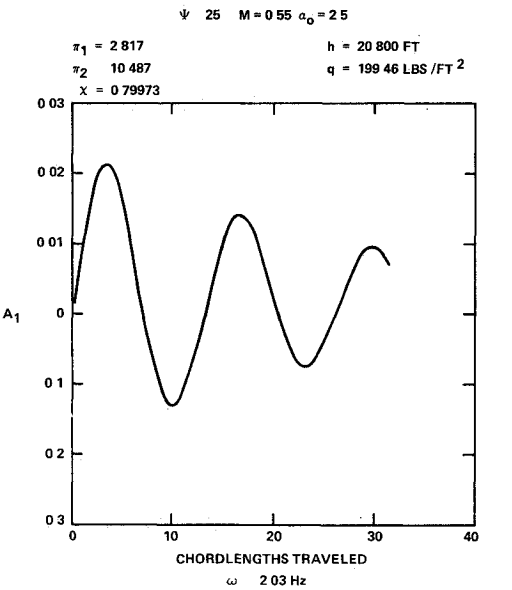

Fig 9 B 1 structurally coupled calculation: $\psi = 25$ deg; $M_\infty = 0\ 55$; $\alpha_0 = 2\ 5$ deg

Figure 10 pertains to the B 1 supercritical condition with strong trailing edge shock, for which the steady state chord wise pressures are indicated in Fig 3 Although an oscillation trace was not available for this condition flutter has been reported in flight The simplified theoretical model used here predicts damped rather than the observed amplified motions at this $\psi = 25$ deg, $M_\infty = 0\ 73$ condition It should be noted however that rather than having a spatially modal character resembling the first free fundamental this case was ex perimentally observed to be more similar to the second mode Since the model described here is based on the assumption of a temporally modulated free fundamental mode, some discrepancy seems to be reasonable in this case Figure 11 corresponds to the B 1 supercritical condition with an oblique trailing edge shock for which the static aerodynamic solution is indicated in Fig 4 An oscillation trace is available for this case, and the simplified theoretical model used here does predict the observed flutter characteristics The calculation predicts a flutter frequency of 2 86 Hz whereas 2 1 Hz was

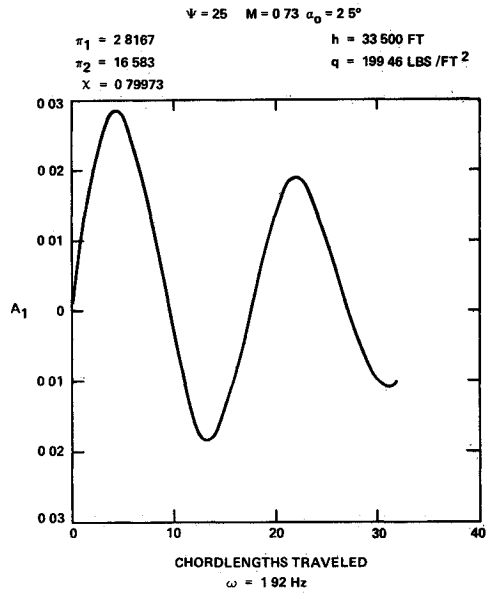

Fig 10 B-1 structurally coupled calculation: $\psi = 25$ deg; $M_\infty = 0\ 73$; $\alpha_0 = 2\ 5$ deg

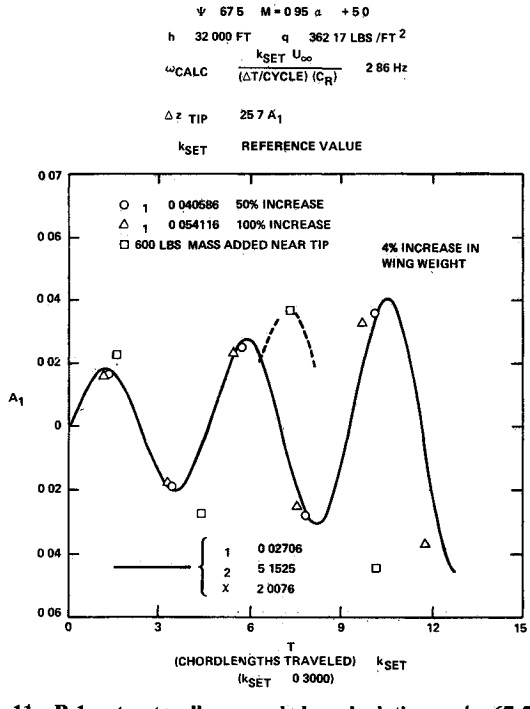

Fig 11 B 1 structurally coupled calculation: $\psi = 67\ 5$ deg; $M_\infty = 0.95$; $\alpha_0 = +5\ 0$ deg

measured in flight This prediction is strongly dependent on the sweep term in the boundary conditions, since when χ is set equal to zero holding everything else fixed, the oscillation had a tendency to damp out

Oscillation peaks for several variations away from the B 1 flutter conditions are indicated by the symbols in Fig 11 As potential fixes, increases of 50% and 100% in wing stiffness or reductions in dynamic pressure (Π_1 increases of 50% and 100%) reduced the amplitude and increased the frequency As another potential fix, a 600 lb mass added near the wing tip increased the amplitude and reduced the frequency

Turning now to the HiMAT, the structurally coupled response for the canard wind tunnel model is shown in Fig 12 It is evident from the figure that the simplified theoretical model predicts a frequency of 57 2 Hz as compared with the measured frequency of 56 0 Hz

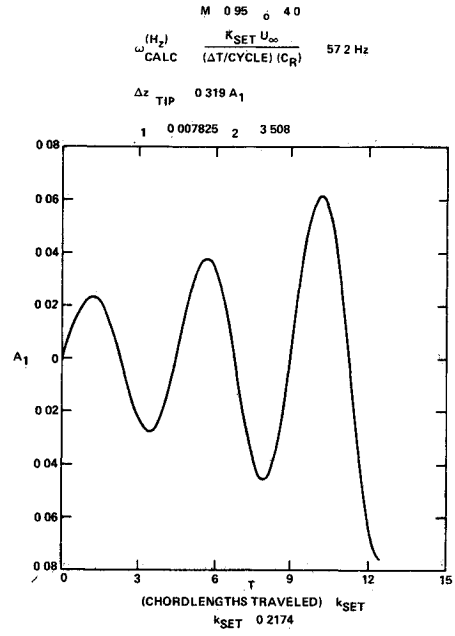

Fig 12 HiMAT structurally coupled calculation: $M_\infty = 0\ 95$; $\alpha_0 = -4\ 0$ deg

The proximity of the flutter frequency to the fundamental for both HiMAT and B 1 cases can be appreciated from a crude order-of magnitude comparison of stiffness and aerodynamic forces If EI is a typical sectional modulus, and the chord c is used as a typical linear dimension, the elastic restoring force is of the order of EI/c^2. Correspondingly, an aerodynamic force is of the order $\rho U^2 c^2$, where ρU^2 is the usual dynamic pressure

The ratio λ of stiffness to aerodynamic forces for the B 1, $\psi = 67\ 5$ deg, in Fig 11 is

$$\lambda \equiv \frac{EI}{U^2 c^4} = \frac{1\ 562 \times 10^9}{(0\ 0008264)(859{,}421)(197{,}899)} = 11\ 1 \quad (16)$$

which is apparently large enough to support the hypothesis of flutter frequency close to the fundamental.

It should be noted that these frequencies are considerably lower than the flutter solutions generated from the linear perturbation model (LSM) discussed in Ref 3 We conjecture that the amplitude of the initial kick ϵ in Eq (13b) can play an important role in this comparison, as can the low frequency dependence of $\tilde{L}$ in Eq (1a) on A_1 and its temporal derivatives. We envision the possibility of limit cycle phenomena and other nonlinear effects also playing a part in the relationship of the perturbation flutter solution of Ref 3 and the fully coupled model The relationship of linear and nonlinear stability characteristics requires further in vestigation in the future

The B 1, $\psi = 67$ 5-deg sweep case of Fig 11 was rerun with Π_2 increased by a factor of 10 0 as a numerical experiment. Flutter is still predicted by the theoretical calculation but the frequency is substantially reduced, as indicated in Ref 3

For the B 1 with 67 5 deg sweep, the flutter condition was reached in a wind up turn at a lower angle of attack From the definition if Π_1 and Π_2 given previously, it is apparent that they are invariant with the angle of attack A typical response at lower angles of attack is shown in Fig 13, corresponding to aerodynamic solutions at these reduced incidence This lower angle of-attack case shows a diverging oscillation and predicts flutter For the B 1 with 67 5 deg sweep, the simplified theoretical model predicts flutter over wider angle of attack and Mach number ranges than were observed in flight Part of this discrepancy may be due to viscous interactions and

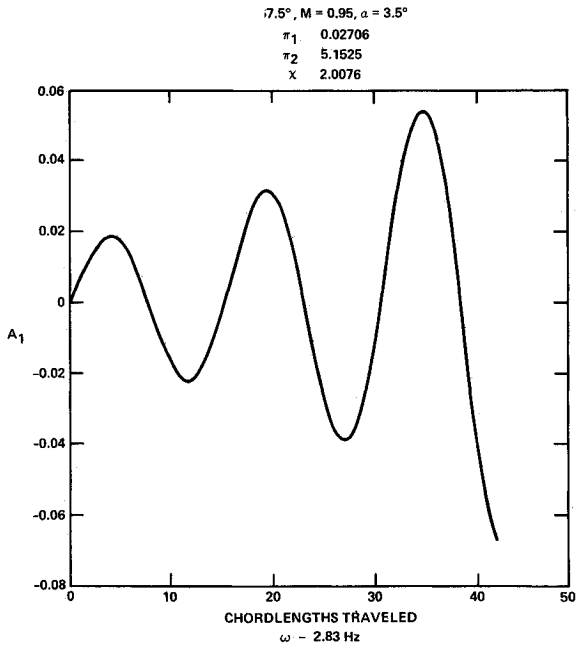

Fig. 13 B-1 structurally coupled calculation: $\psi = 67.5$ deg; $M_\infty = 0.95$; $\alpha = 3.5$ deg.

three-dimensional effects. A discussion of the former is given in Refs. 3 and 4.

Conclusions and Recommendations

On the basis of the model described, the following observations can be made:

1) The NCM provides an accurate prediction of transonic flutter frequencies associated with two out of three nonclassical instability points for the B-1 and HiMAT observed experimentally

2) The NCM correctly predicts the divergence features of the wing displacement on a qualitative basis.

3) Items 1 and 2 are consistent with a structural dynamic model of the wing in nearly free bending with weak aerodynamic negative damping. Actual parametric values for these cases are also consistent with this picture.

4) For the third point, where damped rather than experimentally observed amplified oscillations are predicted, one source of discrepancy is that the model assumes a temporal modulation of the free fundamental spatial mode, whereas the observed modulation was on the second mode.

5) Sweepback has a destabilizing effect.

6) Increases of 50 and 100% in wing stiffness or reductions in dynamic pressure of these amounts reduce the amplitude and increase the frequency of the response in the NCM model.

7) Addition of a wing-tip mass increases the amplitude and reduces the frequency of the response.

8) The angle-of-attack range for which the divergence was experienced in the analytical model was much broader than that observed. This may be due to viscous and three dimensional effects.

Future effort should be devoted to relaxing the assumptions of strip theory relevant to high-aspect-ratio shapes and to studying approximate three-dimensional formulations for the aerodynamic module. This is particularly relevant to the $\psi = 0(\delta^{1/3})$ assumption and to applications of the NCM to the B-1, $\psi = 65$-deg case, and is significant in improving correlations with experiment. For low-aspect-ratio fighter shapes, such as the HiMAT the transonic unsteady equivalence rule described in Ref. 15 may be useful. In addition, limit cycle aspects associated with the role of the ϵ parameter and the steady-state static equilibrium conditions should be investigated. Finally, NCM refinements should include the influence of modal coupling and static flexibility

Acknowledgments

The research described in this paper was sponsored under Contract, F33615-80-C 3208, "Investigations of Structural Dynamic Instabilities in Transonic Flow" by the Flight Dynamics Laboratory, AFWAL/FIBRC, Air Force Wright Aeronautical Laboratories, Wright-Patterson Air Force Base, Ohio. In this connection, the authors wish to thank S. Pollock, D. Cooley, and J. Olsen for valuable interactions with respect to this program. In addition, they wish to acknowledge the assistance of P Goorjian of NASA-Ames Research Center in connection with supplying the LTRAN2 monotone switch update cards for the parametric studies described herein, and to extend gratitude to B. Engquist and S. Osher for help in implementation of their monotone switch procedure. Finally, appreciation is expressed for the transmittal of B-1 and HiMAT data used in this study from G. D. Miller and R. Nishida of Rockwell's North American Aviation Division.

References

[1] Stevenson, J. R., "Shock Induced Self-Excited Airfoil Bending Oscillations," Los Angeles Rockwell International, paper presented to Aerospace Flutter and Dynamics Council, Las Vegas, Nev., Oct. 19-20, 1978.

[2] Stevenson, J. R. and Malmuth, N. D., "Shock Induced Self-Excited Wing Bending Oscillations," Open Forum Presentation, AIAA/ASME/ASCE/AHS 21st Structures, Structural Dynamics and Materials Conference, Seattle, Wash., May 12-14, 1980.

[3] Malmuth, N. D., Cole, J. D., Chakravarthy, S., and Goebel, T P., "Investigation of Structural Dynamic Instabilities in Transonic Flow," Air Force Flight Dynamics Laboratory, Wright Aeronautical Laboratories, Wright-Patterson AFB, Ohio, Final Report, AFWAL TR-82-3003, Feb. 1982.

[4] Malmuth, N. D., Chakravarthy, S. R., Cole, J. D., and Goebel, T P., "Bending Effects on Structural Dynamic Instabilities of Transonic Wings," AIAA Paper 83-0920, May 1983.

[5] Ballhaus, W F and Goorjian, P. M., "Computation of Unsteady Transonic Flows by the Indicial Method," *AIAA Journal*, Vol. 16, Feb. 1978, pp. 117-124.

[6] Yang, T. Y., Guruswamy, P., and Striz, A. G., "Flutter Analysis of a NACA 64A006 Airfoil in Small Disturbance Transonic Flow," *Journal of Aircraft*, Vol. 17 April 1980, pp. 225-232.

[7] Isogai, K., "Numerical Study of Transonic Flutter of a Two-Dimensional Airfoil," National Aerospace Laboratory, Tokyo, Japan, Report NAL TR-617T, July 1980.

[8] Borland, C. J., Rizzetta, D., and Yoshihara, H., "Numerical Solutions of Three-Dimensional Unsteady Transonic Flow over Swept Wings," *AIAA Journal*, Vol. 20, March 1982, pp. 340-347

[9] Ashley, H., "Role of Shocks in the 'Subtransonic' Flutter Phenomenon," *Journal of Aircraft*, Vol. 17 March 1980, pp. 187-197

[10] Tijdeman, H., "On the Motion of Shock Wave on an Airfoil with Oscillating Flap," *Symposium Transsonicum II*, Springer-Verlag, Berlin, 1975, pp. 49-56.

[11] Engquist, B. and Osher, S., "Stable and Entropy Satisfying Approximations for Transonic Flow Calculations," *Mathematics of Computation*, Vol. 34, 1980, pp. 45-75.

[12] Goorjian, P M. and von Buskirk, R., "Implicit Calculations of Transonic Flow using Monotone Methods," AIAA Paper 81-331, 1981.

[13] Yates, E. C. Jr., Wynne, E. C., and Farmer, M. G., "Effects of Angle of Attack on Transonic Flutter of a Supercritical Wing," *Journal of Aircraft*, Vol. 20, Oct. 1983, pp. 841-847

[14] Edwards, J. W., Bennett, R. M., Whitlow, W Jr., and Seidel, D., "Time Marching Transonic Flutter Solutions Including Angle of Attack Effects," *Journal of Aircraft*, Vol. 20, Nov. 1983, pp. 899-906.

[15] Malmuth, N. D., Wu, C. C., and Cole, J. D., "Slender Body Theory and Optimization Procedures for Transonic Wing-Bodies," AIAA Paper 83-0184, Jan. 1983.